ELECTRONICALLY CONTROLLED REACTIONS OF INTERSTITIAL IRON IN SILICON

L.C. KIMERLING and J.L. BENTON

Bell Laboratories, Murray Hill, New Jersey 07974, U.S.A.

The association and dissociation reactions of the interstitial iron-substitutional boron pair (Fe_iB_s) in silicon have been studied by capacitance transient techniques. Electronic mechanisms play a role in both reactions. The deep donor state of (Fe_i) , H(0.46), is critical to the phenomena by providing 1) a charge state controlled ion pair relaxation process, and 2) charge localization and electron-phonon coupling which support the recombination enhanced motion of (Fe_i) . The projected lattice potentials experienced by (Fe_i^*) in the vicinity of (B_s^-) are derived from the reaction kinetics.

1. INTRODUCTION

Transition metal impurities in silicon represent an intriguing system for defect studies. The observation of trends in the chemical and electronic behavior of these elements as a function of delectron occupation presents an opportunity to probe both electron-lattice and electron-electron interactions in covalent systems. In general, these impurities can occupy both the substitutional and the tetrahedral interstitial lattice sites, and they introduce multiple electronic states in the band gap. 1 This dual behavior suggests this system as a candidate for electronically driven defect reactions. The photodissociation of the iron-boron pair in silicon by white light at 300°K has been recently reported. Similar behavior of an iron-related luminescence spectrum has also been observed. It has been suggested that these phenomena are derived from a direct photon-defect interaction. Our recent work has revealed a linear correlation between the dissociation rate of the (Fe_1B_1) pair and the minority carrier injection current density. We report here the detailed nature of this electronically stimulated reaction and the implications regarding a recombination enhanced diffusion mechanism for isolated interstitial iron.

2. EXPERIMENT

The reactions of iron and boron were studied with capacitance transient spectroscopy by monitoring the respective defect states H(0.10) and H(0.46). The samples consisted of p-type, <100>, float-zoned silicon with boron doping in the range of $10^{13}-10^{16}\ cm^{-3}$. Iron was introduced into the silicon by scraping a piece of high purity wire on both surfaces and heat treating by Rapid Thermal Annealing (quartz lamp illumination) at 1200 °C for 5 seconds in a flowing argon ambient. Schottky barrier structures were constructed by Ti evaporation through a metal mask at room temperature after processing. P-n junction samples were formed by implantation of 50 keV arsenic to a dose of $10^{15}\ cm^{-2}$ prior to processing. Mesa junctions were defined after heat treatment by aluminum metallization followed by sand blasting and etching. The dominant feature in the resulting DLTS spectrum was in all cases H(0.10), the (Fe_iB_s) pair state.

3. RESULTS

The properties of interstitial iron were explored by monitoring the association and dissociation kinetics of the pairing reaction

$$(Fe_i)^+ + (B_s)^- \stackrel{\longrightarrow}{=} (Fe_iB_s)^o \tag{1}$$

As previously discussed, 6 the association time constant can be expressed in closed form for an ion pair, Coulomb interaction potential as

$$\tau = \frac{\epsilon kT}{4\pi q^2 D(Fe_i) [B_s]}$$

$$= \frac{557 T}{D(Fe_i) [B_s]}$$
(2)

At elevated temperatures, the electrostatic, pair binding energy is countered by the available thermal energy, and the reaction (1) is driven to the left, dissociation. The fraction of Fe_i which is paired as (Fe_iB_s) at a given temperature is determined by the relation

$$f = \frac{[B_s]}{Z N} \exp(E_b/kT)$$
 (3)

$$=5 \times 10^{-24} [B_s] \exp (E_b/kT)$$

where N is the lattice site density in silicon $(5 \times 10^{22} cm^{-3})$, Z is the number of pair configurations about one site (4 for the tetrahedral interstitial site), and E_b is the electrostatic pair binding energy which should be the order of 0.5 eV for two point charges in silicon, located at the tetrahedral interstitial and substitutional sites, respectively.

In the following, we explore the mechanisms by which the rates of the association and dissociation reaction can be controlled electronically rather than thermally.

3.1 Association: Charge State Effects

The association reaction is driven by the Coulomb attraction between the positively-charged interstitial iron and the negatively-charged, acceptor boron. If one of the partners becomes neutral, the pairing reaction is quenched. In p-type material, this change in charge state can be accomplished by placing the Fermi level below the boron acceptor level, E_{ν} +0.045 eV, or above the interstitial iron donor level, E_{ν} +0.39 eV. The latter process is most conveniently effected by applying a reverse bias to the sample structure. This action nominally pins the Fermi level at midgap within the spatial extent of the depletion region. Thus, the interstitial iron donor state will be empty of holes or charged neutral.

Figure 1 shows a comparison of the decay rates of the interstitial iron signal, H(0.46) at 296 K under conditions in which a reverse bias of -10v was applied and under zero biased, shorted diode conditions. Changing the charge state of (Fe_i) from +1 to 0 has clearly extinguished the pairing reaction. One can conclude from this result that pair formation will not occur in n-type material, even when significant background acceptor (boron) concentrations are present.

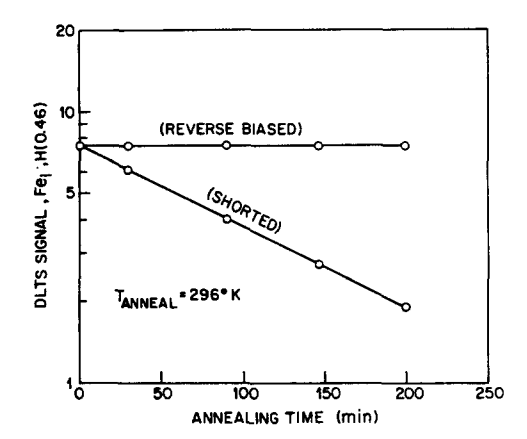


Figure 1. Influence of (Fe_l) charge state on the pair association rate. Under reverse bias, the charge is (Fe_l^o) within the depletion region. At zero bias, the Fermi level is positioned below H(0.46) and the charge state is (Fe_l^{\dagger}) .

Pair stability should be similarly influenced by the charge of the constituents. If the pair is a simple association of two point charges, the defect states observed in the gap represent perturbed (Fe_l) levels. This conclusion is based on the fact that a nearby charge of opposite sign will push the boron acceptor level into the valence band and the interstitial iron donor level toward the conduction band. Thus, the (Fe_lB_s) pair, H(0.10) donor state represents the +/++ double donor state of (Fe_l) .

A deeper state near midgap has also been reported for the (Fe_iB_s) pair. 12 , 13 This level would correspond to the (Fe_i) donor, o/+ state. Evidence for the existence of such a state is found in the observation that the room temperature reverse recovery, lifetime in these samples is lowered by a factor of four in the paired state relative to the free (Fe_i) condition. 14 The shallow H(0.10) state cannot be responsible for this result.

One can construct from the above, a Fermi level diagram for use in predicting the electronic conditions for pair formation and stability. A schematic drawing is given in Figure 2. The shaded areas denote the Fermi level positions for which the association reaction occurs and for which the pairs, once formed, are stable. Favorable thermal conditions (e.g., 300 K) for diffusion and pair binding are, of course, assumed.

3.2 Dissociation: Recombination Enhanced Motion

The equilibrium fraction of pairs at a given temperature is defined by Equation (3). Measurement of the paired fraction as a function of temperature 15 has yielded the quantitative relation

$$\frac{(Fe_i \ B_s)}{(Fe_i)(B_s)} = 10^{-23} \exp\left[\frac{0.65 \pm 0.02 \ eV}{kT}\right]. \tag{4}$$

This result is in good agreement with similar measurements, recently reported by Lemke. ¹³ The measurements confirm that, for $(B_s) > 10^{14} \ cm^{-3}$, almost all of the iron is stable as (Fe_iB_s) at temperatures below 300° K. However, this equilibrium can be perturbed by irradiation with white light or minority carrier injection. These nonequilibrium processes have been studied in detail.

At any temperature above 77°K the dissociation reaction can be driven to greater than 95% completion by injection of minority carriers. Thus, not only is the dissociation rate enhanced, but the

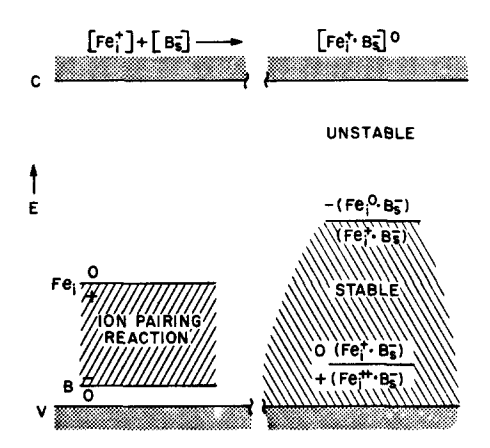


Figure 2. Stability diagram for (Fe_iB_s) ion pairs. The shaded areas denote Fermi level positions for which a) the association reaction will occur, and b) the nearest neighbor pairs are bound.

association process is retarded. The capture of injected electrons by $(Fe_i)^+$ yields a neutral or negative entity which will not participate in the ion pairing process. The mobile species, therefore, is not expected to engage in pair formation.

The rate of injection enhanced dissociation is directly proportional to the injected current density. Figure 3 shows a comparison of the dissociation rates observed under thermal and electronic stimulation. The injection enhanced data has been normalized to a

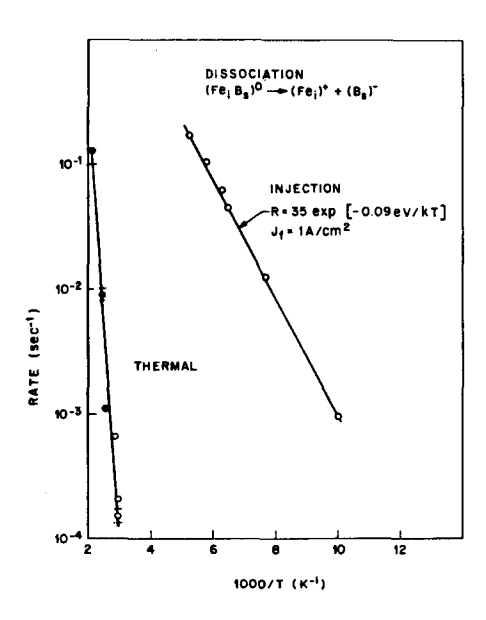


Figure 3. Dissociation rate of the (Fe_iB_s) pair. The injection annealing rates increase linearly with current density.

1A/cm² injection current density. It is notable that the injection stimulated process exhibits both a reduced activation energy and a reduced preexponential factor. Both of these features are common to recombination enhancement. where electronic energy is converted into local vibrational energy and the attempt frequency corresponds to the electron-hole recombination rate. The observed temperature dependence of the injection mechanism is consistent with the prior observation that the photostimulated process is active at 300°K but slow or nonexistent at 77°K.

The effectiveness of minority carrier injection in stimulating the long-range diffusion of isolated (Fe_i) as opposed to a single jump (Fe_iB_i) pair dissociation event can be explored through the diffusion limited association kinetics. Figure 4 shows the association rates for a variety of samples as a function of temperature, normalized to a B_i acceptor concentration of $3\times10^{15}\,cm^{-3}$. The data were taken following dissociation by heat treatment at 200° C for 10 minutes or by forward bias injection at $5A/cm^2$, 300° K for 5 minutes. The identity of the recovery rates in both cases means that the (Fe_i) concentration has been randomized by long-range diffusion with electronic stimulation as with the thermal treatment. This is the first direct observation of electronically enhanced diffusion by an isolated impurity. The corresponding behavior for Cu and Ni is currently under study.

The lattice potentials in the vicinity of the (Fe_iB_3) pair can be studied by limiting the (Fe_i) diffusion to near neighbor positions. This state can be prepared by injection for short times at low temperatures where enhanced rate is reduced (Fig. 3). Figure 5 shows the temperature dependence of the initial rate of pair formation following injection of $0.5 \text{A}/\text{cm}^2$ for 100 seconds at 130° K. 18 The recovery rate is faster by approximately five orders of magnitude than the process reflecting long range diffusion (Figure 4). This result is consistent with the reduction in the number of required diffusion jumps.

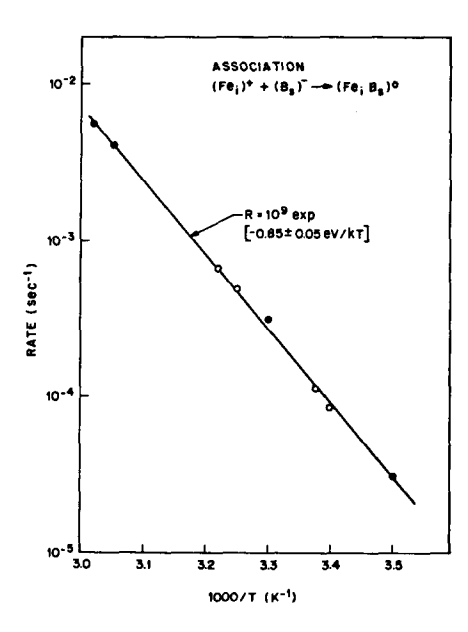


Figure 4. The association reaction kinetics for (Fe_1B_s) . The filled circles represent data taken after thermal dissociation at 200°C, 10 minutes. The empty circles represent data following electronic dissociation $I_F = 5A/cm^2$ at 300°K, 5 minutes.

The reduced activation energy, $0.65 \pm .05$ eV relative to $0.85 \pm .05$ eV, is a reflection of the Coulomb envelope impressed on the lattice potential by the electrostatic pair interaction. The preexponential factor is in the range expected for a single jump process (i.e., the lattice vibration frequency, $10^{12}-10^{13}\,sec^{-1}$). The absence of a charge state (diode bias) effect in the data of Figure 5 is unexpected. The driving force for the pairing reaction is predominantly electrostatic. The equilibrium data suggest, however, that the binding energy is enhanced by about 0.1 eV by an additional interaction. A tensile strain associated with the under-

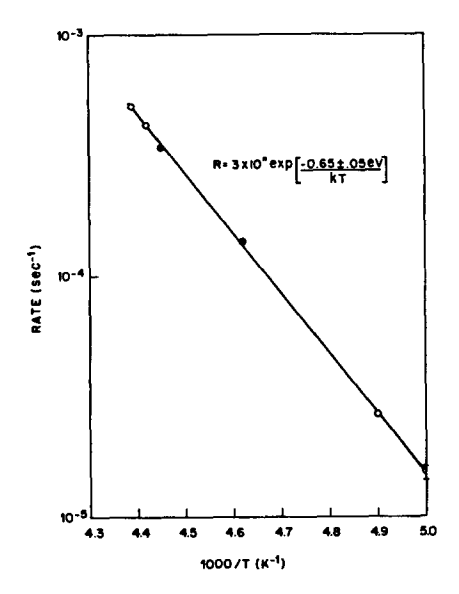


Figure 5. Pair formation rate for second nearest neighbor (Fe_i) and (B_s). The data were taken following dissociation at 130°K, $I_F = 0.5A/cm^2$, 100 seconds. The empty circles represent data taken at $V_R = 0V$, filled circles, $V_R = -10V$.

sized boron atom could provide an attractive potential relative to the compressive strain of the interstitial iron. Thus, at the nearest neighbor site, a short range interaction may be operative, independent of charge state. The alternative explanation is that the defect states of the nearest neighbor constituents are not simple Coulomb perturbations of the free Fe_l and B_s states, i.e. are not positioned between H(0.1) and midgap.

A schematic diagram of the projected lattice potential near the (Fe_iB_s) pair based on the results presented here is shown in Figure 6. The pair formation rate data yields a migration energy for isolated (Fe_i) of $E_m = 0.85 \pm 0.05 \ eV$. The pair equilibrium studies show a binding energy of $E_b = 0.65 \pm 0.02 \ eV$ which defines the Coulomb envelope near the boron acceptor.

4. DISCUSSION

The ion pair $(Fe_i^+B_i^-)$ is shown to respond as a classic system consisting of a mobile, positively charged donor and a fixed negative acceptor embedded in a dielectric medium. The deep donor state of (Fe_i) gives rise to two new phenomena: 1) a charge state controlled pair relaxation process; 2) charge localization and electron-phonon coupling which allow recombination enhanced motion of (Fe_i) at low temperatures.

THE IRON-BORON PAIR IN SILICON

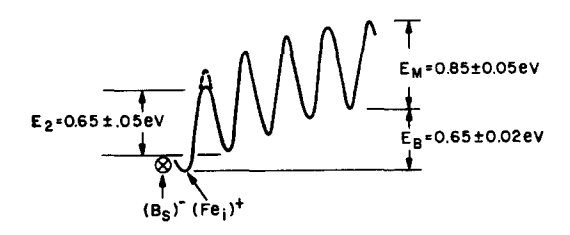


Figure 6. Schematic diagram of lattice potentials for (Fe_i^+) near (B_s^-) . E_m is the free (Fe_i^+) migration enthalpy observed in the association reaction (Fig. 4). E_b is the $(Fe_i^+B_s^-)$ pair binding energy derived from the equilibrium studies (Eq. 4). E_2 is the single hop barrier to second neighbor (Fe_i^+) for pair formation (Fig. 5)

The recombination driven pair dissociation is characterized as an energy deposition process by the observed kinetics and the energy barrier involved. If the charge on (Fe_i) is merely neutralized, an ≈ 0.9 eV barrier must still be surmounted to yield dissociation. The room temperature rate for this process would be less than 10^{-3} sec⁻¹. Even if Coulomb repulsion were introduced by a negatively charged (Fe_i) , the observed long range motion could not be explained.

The recombination rate at the (Fe_iB_s) centers under $1A/cm^2$ injection is estimated to be $R_R = 10^7 - 10^8 \ sec^{-1}$. Consider the preexponential factor as $\eta \ R_R/N_j$ where η is the fraction of recombination events producing a diffusion jump and N_j is the number of jumps required to produce a stable separated pair. For $N_j \simeq 10^1 - 10^2$, the observed value of 35 indicates $\eta = 10^{-5}$. Assuming that electron capture neutralizes the (Fe_i) , the relevant reduction in the apparent activation energy is that of (Fe_i) diffusion, from $E_T = 0.85 \pm .05$ eV to 0.09 eV. This enhancement is consistent with electron capture from the conduction band by the H(0.1) donor state of $(Fe_i)_s$, $E_R \simeq 1$ eV, or by the H(.46) donor state of $(Fe_i)_s$, $E_R \simeq 0.8$ eV. Thus, recombination enhancement can support both the dissociation and migration processes.

Whereas the spectral dependence of the photostimulated process was not explored in detail, the reported temperature dependence is consistent with white light acting as a source of minority carrier injection for the process described above.

In summary, electronic mechanisms can control both the association and dissociation reactions of the (Fe_lB_s) pair. In both cases, the basis for the mechanism is electronic transitions at the (Fe_l) impurity site. The recombination enhanced motion of the isolated impurity is indeed remarkable. Trends in the related behavior across the 3d transition metal family are being explored.

REFERENCES

- [1] Ludwig, G. W. and Woodbury, H. H., Solid State Physics 13 (1962) 223.
- [2] Graff, K. and Pieper, H., J. Electrochem. Soc. 128 (1981) 669
- [3] Weber, J. and Wagner, P., Proc. 15th Int. Conf. Physics of Semiconductors, Kyoto, 1980, J. Phys. Soc. Japan 49 (1980) Suppl. A, 263.
- [4] Corbett, J. W., Jaworowski, A., Kleinhenz, R.L., Pierce, C. B., and Wilsey, N. D., Solar Cells 2 (1980) 11.
- [5] Kimerling, L. C., Defects in Semiconductors (MRS Proc. 2, North Holland, New York, 1981) 85.
- [6] Kimerling, L. C., Benton, J. L., and Rubin, J. J., Defects and Radiation Effects in Semiconductors 1980 (Inst. Phys. Conf. Ser. 59, 1981) 217.
- [7] Graff, K. and Pieper, H., Semiconductor Silicon 1981 (The Electrochem. Soc., Pennington, N. J., 1981) 331.
- [8] Benton, J. L., Celler, G. K., Jacobson, D. C., Kimerling, L. C., Lischner, D. J., Miller, G. L., and Robinson, McD., Laser and Electron-Beam Interactions with Solids (MRS Proc. 4, North Holland, New York, 1982) 765.
- [9] This level is spectroscopically denoted H(0.46) in this work, reflecting the observed activation energy for hole emission to the valence band of 0.46 eV. This activation energy corresponds to the approximate level position. The reduced value has been determined to be $E_{\nu} = 0.39eV$ by reference 7 and by Wunstel, K. and Wagner, P., Appl. Phys. A27 (1982) 207.
- [10] The DLTS spectra were measured at $V_R = -6V$.
- [11] An alternate reaction in n-type material is the pairing of (Fe_i)⁻ acceptors, if this state exists, with the donor dopant. This associate and/or one involving the (Fe_e)⁻ acceptor have been shown to play a role in the gettering of transition metal contaminants by high concentration phosphorus diffused regions. Meek, R. A. and Seidel, T. E., J. Phys. Chem. Sol. 36 (1975) 731.
- [12] Collins, C. B. and Carlson, R. O., Phys. Rev. 108 (1957) 1409
- [13] Lemke, H., Phys. Stat. Sol. a64 (1981) 215.
- [14] Miller, G. L., private communication.
- [15] Kimerling, L. C. and Benton, J. L., to be published.
- [16] Stimulation of diffusion limited reactions have been reported for (Al_i) and (B_i). However, these species are not equilibrium entities. They are only observed following electron bombardment and are more correctly regarded as defectimpurity complexes.
- [17] Kimerling, L. C., Solid St. Electronics 21 (1978) 1391.
- [18] The observed relaxation is nonexponential because of a distribution of pair separations. Approximately 10% of the (Fe_i) are determined to be in second neighbor positions from the extent of the initial rate. Longer times of the same injection treatment yield 100% distant pairs, confirming the phenomenon of injection stimulated diffusion of isolated interstitial iron.